Electronic Supplementary Material (ESI) for RSC Advances.

Supplementary Information

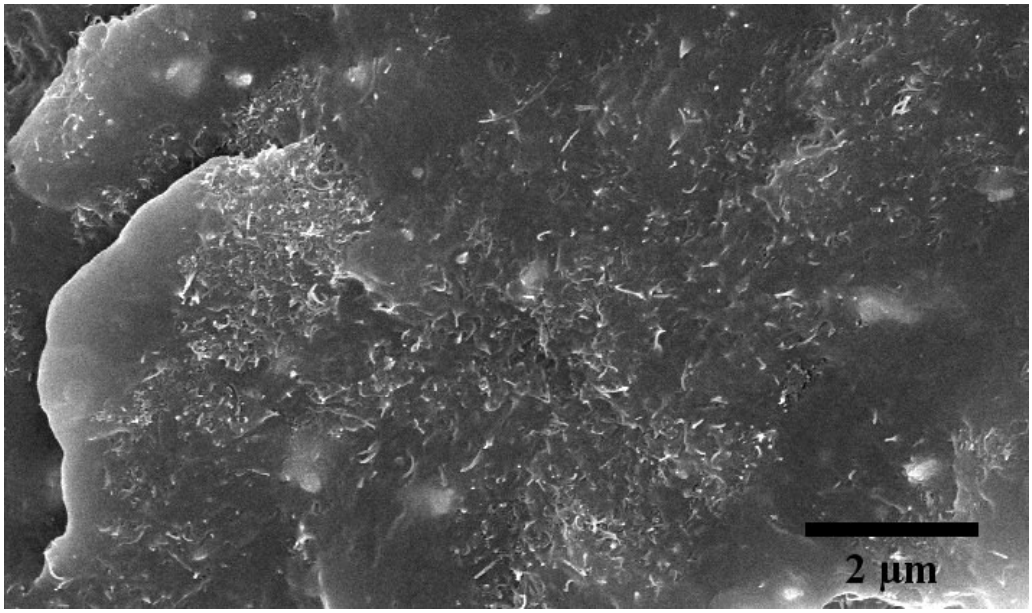

(a)

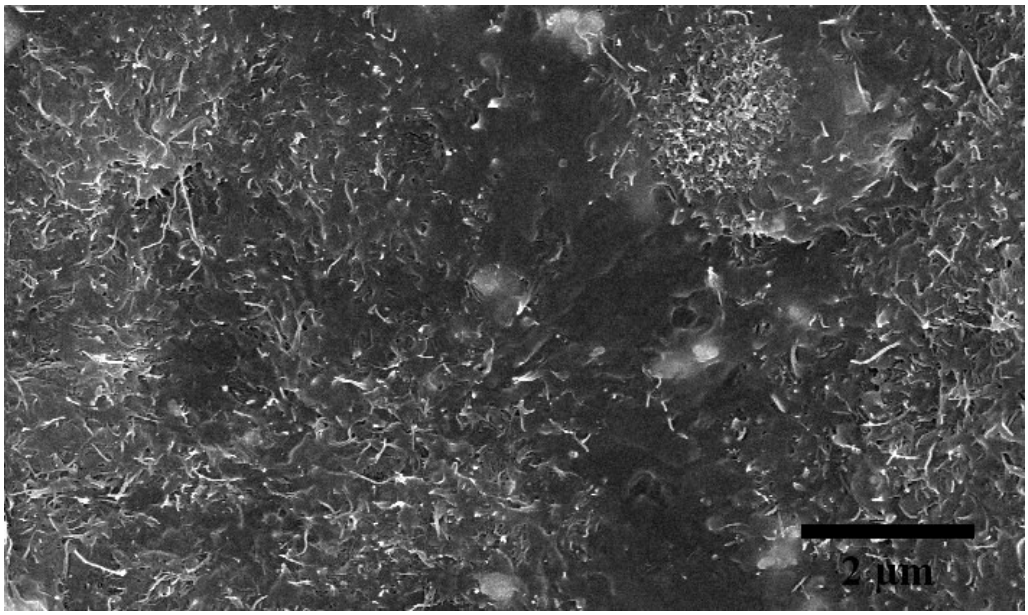

(b)

Fig.S1: SEM images of PVDF+1% MWNT composite (a) and PVDF+2% MWNT composite (b) at a lower magnification showing the dispersion of MWNTs in the PVDF matrix

The WAXD pattern was recorded by Pan- Analytical (Netherlands) X-ray diffractometer with Cu-Kα radiation (λ= 0.154 nm) and a Ni filter with a step size of 0.02°.

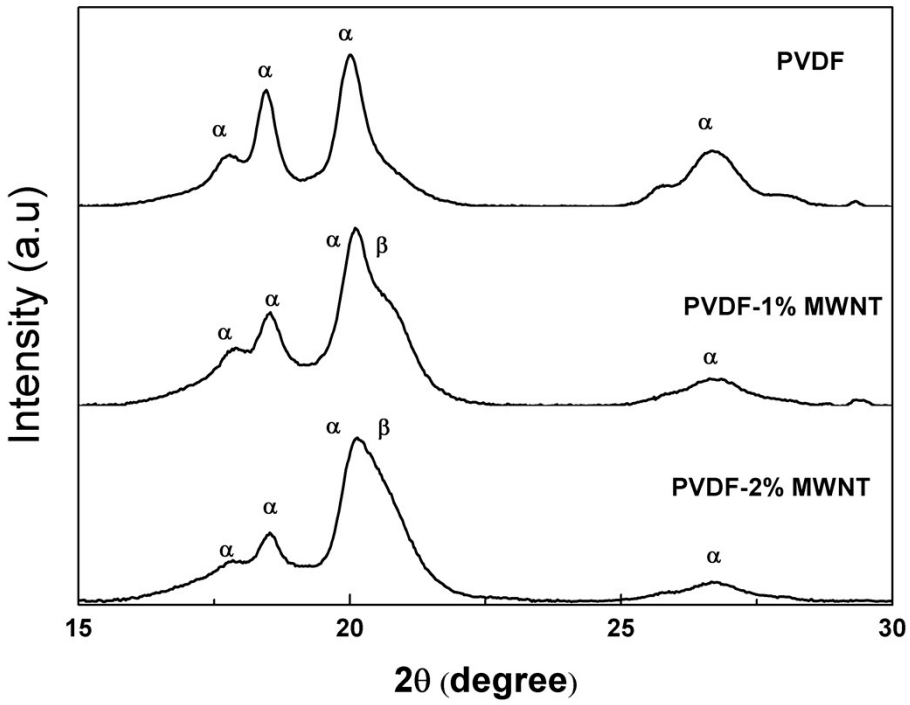

Figure S2: A comparison of WAXD patterns for PVDF-MWNT composites. The amount of β phase is significantly higher in 1 and 2wt. % MWNT composite than in the neat PVDF.

Mechanical Properties: The mechanical properties were determined by uniaxial tensile test of the standard dog-bone shaped samples prepared by hot pressing at 220°C. The tensile response of the samples was measured by an Instron Universal Testing Machine (UTM) at room temperature with crosshead speed of 5 $mm.min^{-1}$. The parameters like Young's Modulus (E), Ultimate tensile strength (UTS) and elongation at break were determined from the stress-strain response of the PVDF-MWNT composites.

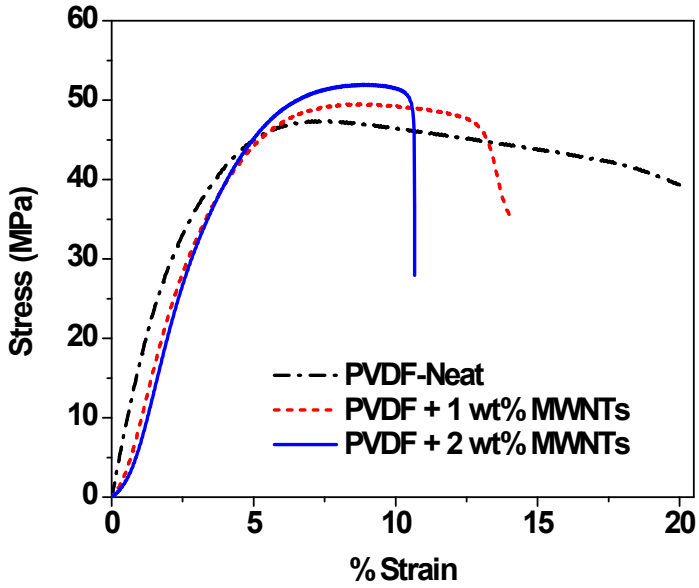

Figure S3: Engineering stress-strain response of PVDF-MWNT composites subjected to uniaxial tension test.

Fig.S3 presents the representative stress-strain response under uniaxial tension. The stress-strain response of PVDF resembles that of a typical polymeric material with a small linear elastic deformation upto the point of yielding, but mostly dominated by viscoelastic deformation. On the other hand, in PVDF-MWNT composites, the initial elastic deformation is similar but the post-yielding deformation at constant stress level is lesser compared to neat PVDF, leading us to presume that this might be due to the restriction in reorientation of

chains in the presence of MWNTs. Another indication of this is the lower percentage elongation at failure.

Crystallization Kinetics: In order to obtain further insight into this role of nanotubes in nucleation and growth of PVDF, we studied isothermal crystallization kinetics of the neat and MWNT filled composites. The well-known Avrami model can be applied to analyze the isothermal crystallization kinetics, as given in equation,[3]

$$X_t = 1 - exp^{(kt^n)}$$

where X_t is the relative crystallinity, n is Avrami exponent, k is crystallization rate constant involving nucleation and growth parameter. Further, the relative crystallinity, X_t can be determined as follows,[4]

$$X_t = \frac{\int_0^t (\frac{\partial H_c}{\partial t}) dt}{\int_0^\infty (\frac{\partial H_c}{\partial t}) dt}$$

where dH_c is the enthalpy of crystallization during infinitesimal time dt.

Fig. S4 shows the plots of X_t – time (t) for PVDF and PVDF+2% MWNT (additional X_t v/s time data for PVDF+1% MWNT is available in supplementary material, Fig. S1). For all the composites, the relative crystallinity curve resembles sigmoidal shape at all crystallization temperatures. The initial step of the '*S*' shaped curve signifies the induction time and nucleation step, followed by a linear part considered as primary crystallization and finally, a nonlinear part attributed to the secondary nucleation caused by the impingement of PVDF spherulites during crystal growth.[4] As observed from the Fig. S4, the sigmoidal curve shifts to the right when the crystallization temperature increased. One of the most important

parameter, $t_{1/2}$ which is defined as the time required to achieve 50% crystallinity can be directly obtained from the Fig. S4 and is listed in table S1. It is evident that for a given composite, higher the crystallization temperature, higher is the $t_{1/2}$. As expected, at higher temperature the growth of spherulites is slower and it is accelerated at lower temperature. It is also supported by the optical images captured using POM Fig.S6 a-c. For neat PVDF, we observe that larger spherulites are grown over longer period of time. In contrast at lower temperatures, smaller spherulites are developed within shorter period of time.[5]

An analysis of Avrami model is further used to study the non-isothermal crystallization kinetics of PVDF and filled composites,

$$ln[-\ln(1-X_t)] = lnk + n\,lnt$$

A plot of $ln[-\ln(1-X_t)]_{vs} lnt$ for a particular crystallization temperature results in a straight line can be obtained with slope of n, the Avrami exponent and lnk as intercept (See Fig.S6). Table S1 summarizes the parameters derived from fitting experimental data following the Avrami model. We observe the value of n > 2 which signifies growth of crystals is almost three-dimensional.[6]

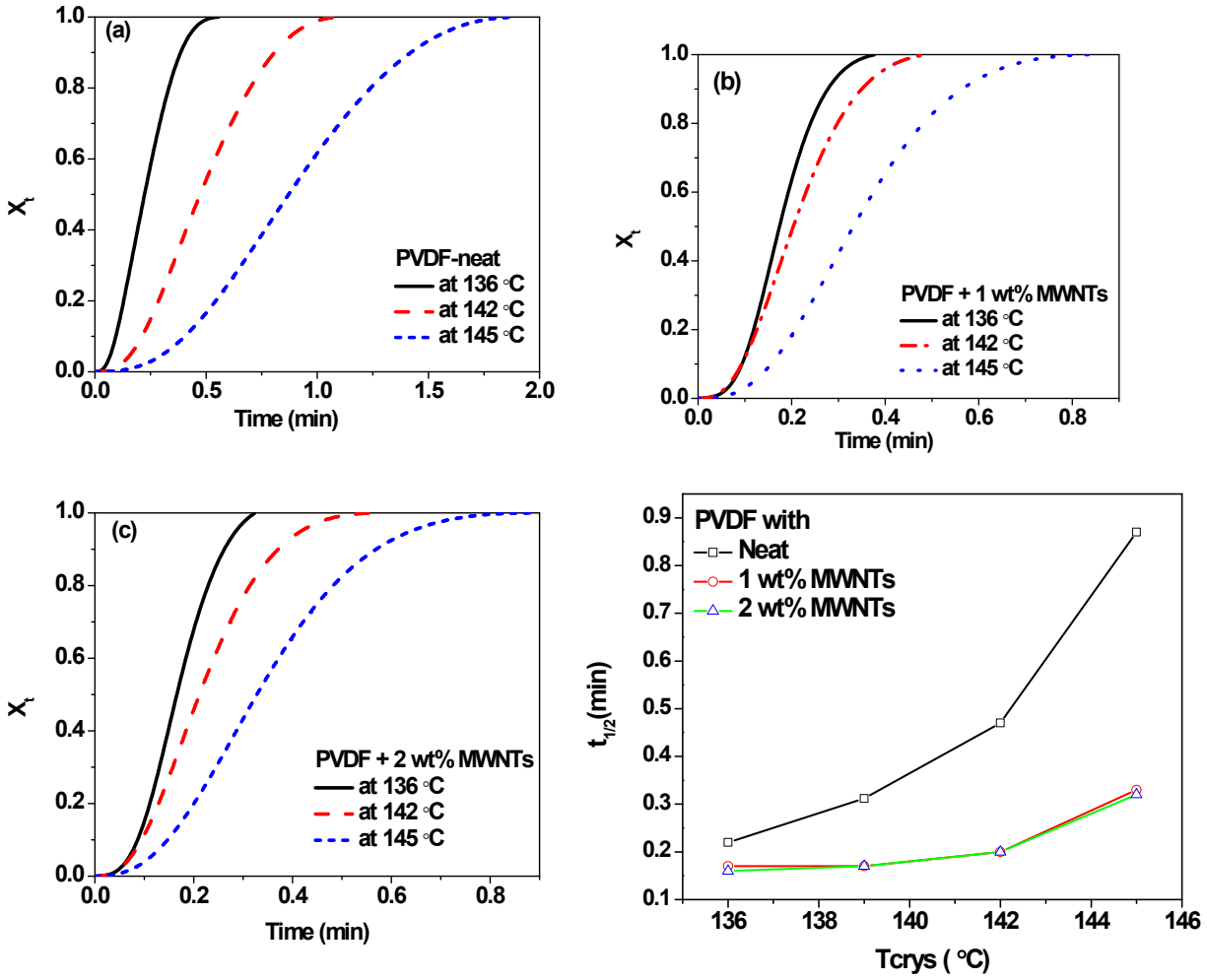

Figure S4: Plots of relative crystanility, X_t vs time of (a) neat PVDF, (b) PVDF + 2 wt% MWNTs, (c) variation of time for 50% crystallization ($t_{1/2}$) with temperature (T_{crys}) for three different blends. The difference in $t_{1/2}$ is higher than at higher T_{crys}.

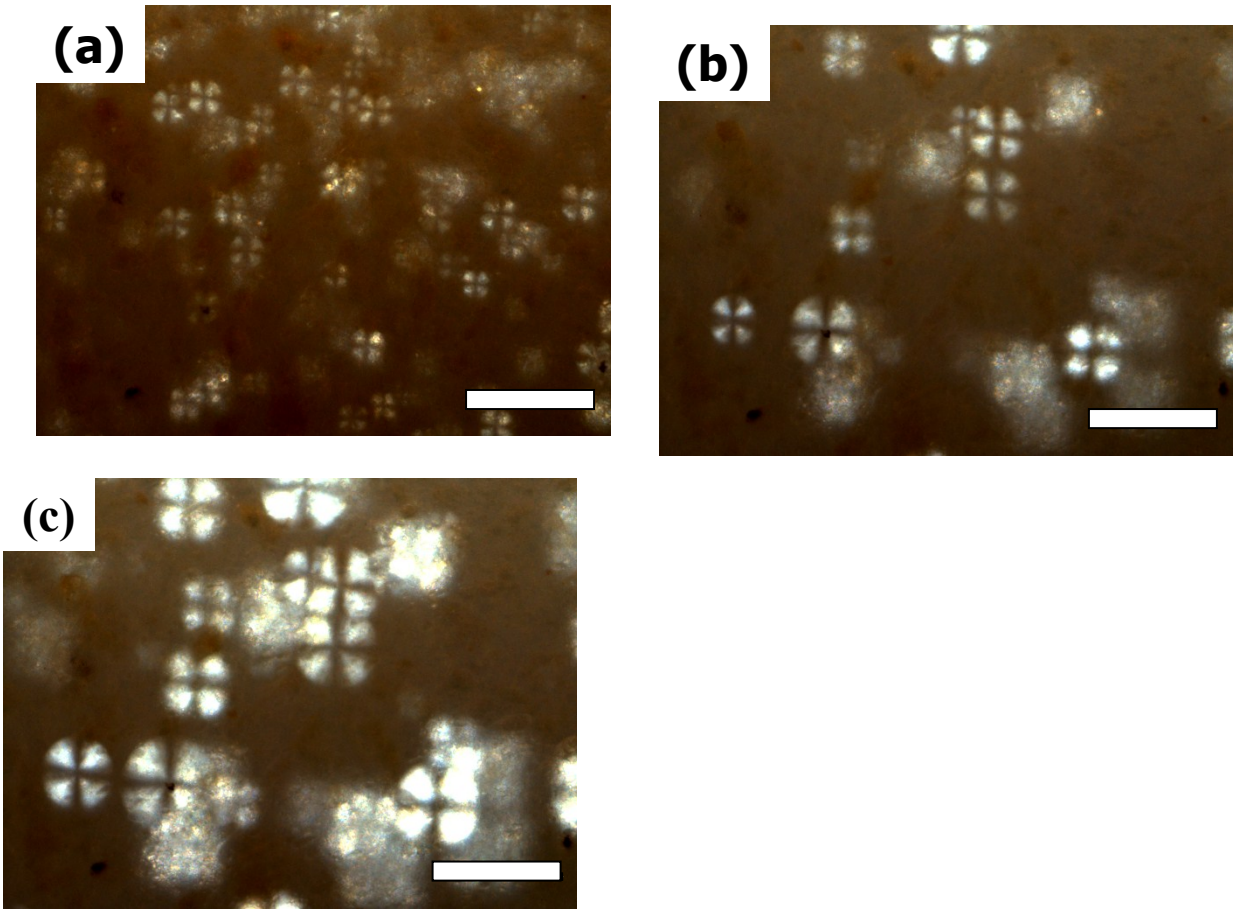

Figure S5 (a-c): Polarizing Optical Microscope image of neat PVDF at three different temperature, (a) 136 °C, (b) 142 °C and (c) 145 °C. The thin film of the composite were heated at 220 °C and then quenched to the corresponding crystallization temperature and maintained isothermal condition. All the images were taken at same time interval. (Scale bar= 100 μm)

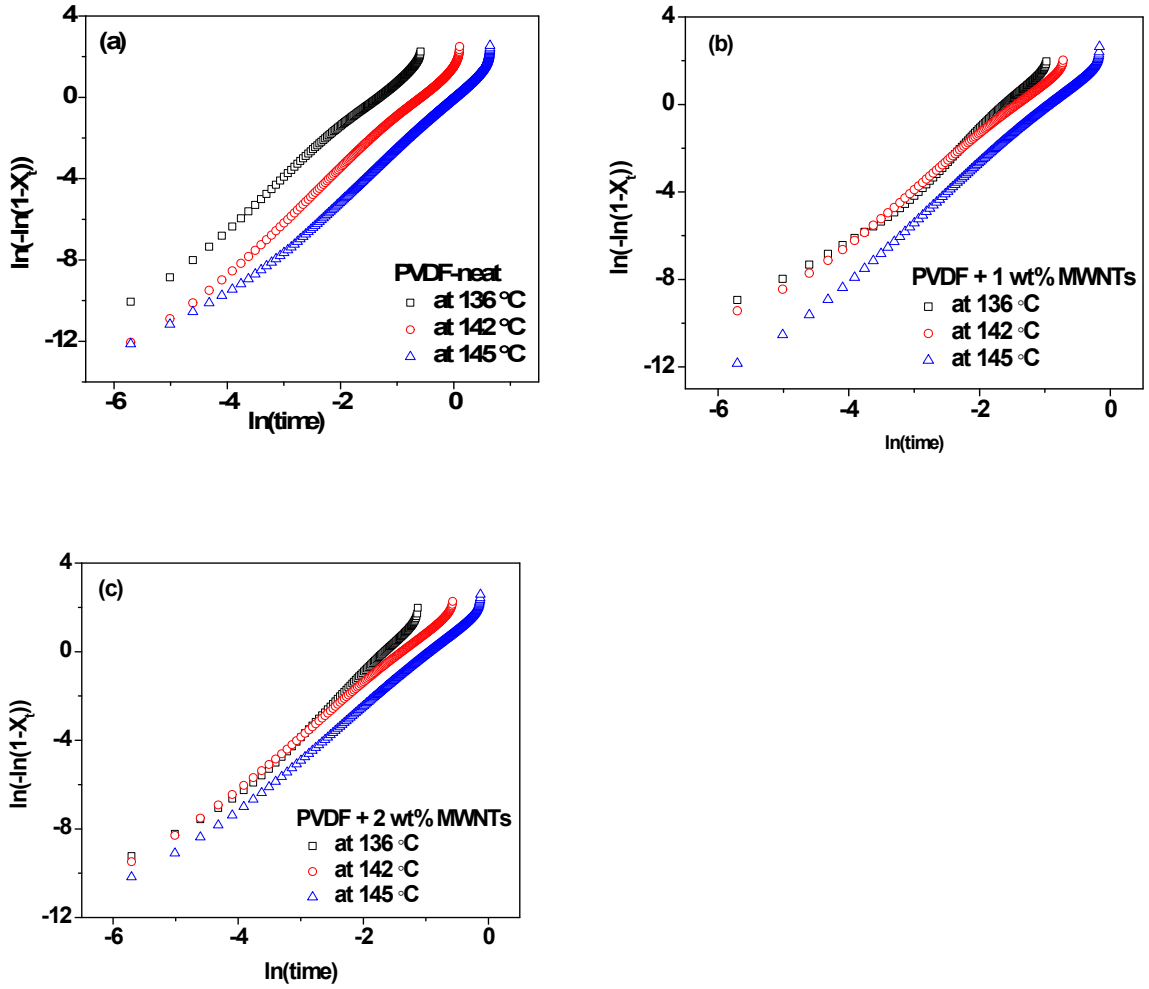

Figure S6: Plots of ln(-ln(1-X_t)) vs ln(time) for (a) neat-PVDF, (b) PVDF+1wt.% MWNT and (c) PVDF+2 wt.% MWNT at three different crystallization temperatures and (d) The trend followed by $t_{1/2}$ for three different temperatures.

Table S1: Parameters derived from Avrami model for crystallization kinetics.

Composite	**T_{crys} (°C)**	**n**	**k (min^{-n})**	**$t_{1/2}$ (min)**
PVDF neat	136	2.6	49.40	0.22
	142	2.7	6.68	0.47
	145	2.6	0.05	0.87
PVDF +1 wt% MWNTs	136	3	121.51	0.17
	142	2.5	7.97	0.2
	145	2.6	4.52	0.33
PVDF +2 wt% MWNTs	136	2.9	134.28	0.16
	142	2.2	18.17	0.2
	145	2.3	9.02	0.32

References

1. G. P. Kar, S. Biswas and S. Bose, *Physical Chemistry Chemical Physics*, 2015, **17**, 1811-1821.
2. Z. Spitalsky, D. Tasis, K. Papagelis and C. Galiotis, *Prog. Polym. Sci.*, 2010, **35**, 357-401.
3. S. Liu, Y. Yu, Y. Cui, H. Zhang and Z. Mo, *Journal of Applied Polymer Science*, 1998, **70**, 2371-2380.
4. A. Durmus, A. Kasgoz, N. Ercan, D. Akın and S. Şanlı, *Polymer*, 2012, **53**, 5347-5357.
5. A. Menyhárd, M. Bredács, G. Simon and Z. Horváth, *Macromolecules*, 2015, **48**, 2561-2569.
6. V. Sencadas, C. M. Costa, J. G. Ribelles and S. Lanceros-Méndez, *Journal of materials science*, 2010, **45**, 1328-1335.